

Cross-Equatorial Response to Middle-Latitude Forcing in a Zonally Varying Basic State¹

PETER J. WEBSTER

Division of Atmospheric Physics, C.S.I.R.O., Aspendale, Victoria, Australia

JAMES R. HOLTON

Department of Atmospheric Sciences, University of Washington, Seattle 98195

(Manuscript received 7 October 1981, in final form 15 December 1981)

ABSTRACT

A nonlinear model based on the shallow water equations is used to study cross-equatorial propagation of forced waves in the presence of a longitudinally varying time-mean basic-state zonal wind field. It is found that global-scale planetary waves are unable to propagate past a critical latitude where the mean zonal wind speed vanishes. However, if the longitudinally-asymmetric basic state includes a "duct" in which the zonal winds are westerly, waves of zonal scale less than the zonal scale of the westerly duct may propagate from one hemisphere to the other even though the zonally-symmetric mean zonal wind remains easterly in the equatorial region. The amplitude of the response in one hemisphere to forcing in the opposite hemisphere increases strongly with the magnitude of the westerlies in the equatorial duct. The existence and annual variations of a westerly duct region in the upper troposphere in the eastern Pacific appear to account for some features of the low-frequency variability in the Northern Hemisphere.

1. Introduction

In his classic paper on tropical scale analysis, Charney (1963) suggested that outside of convectively disturbed regions, tropical perturbations could not originate *in situ* but must be forced either by coupling to midlatitude systems or to convectively active tropical systems. On the basis of a rather idealized linear wave analysis Mak (1969) argued that tropical systems are predominantly driven by midlatitude systems. However, Charney (1969) and Bennett and Young (1971) showed that if a realistic latitudinally-dependent mean zonal wind is included, linear wave calculations suggest that only planetary-scale Rossby waves with easterly phase speeds greater than the maximum easterly mean zonal wind speed in the tropics can propagate meridionally through the tropics. Such modes, argued Charney, would possess insufficient energy to be of significance. Synoptic-scale disturbances, with their characteristically small zonal phase speeds, would propagate equatorward only as far as the *critical latitude* along which the mean zonal wind speed matched the zonal phase speed of the waves.

The behavior of Rossby-mode disturbances propagating meridionally toward a critical line has been

discussed by Dickinson (1970), Geisler and Dickinson (1974), Beland (1976), Warn and Warn (1978), Tung (1979) and others. It still remains a matter of controversy whether Rossby waves are primarily absorbed or reflected at a critical line. But in either case both linear and nonlinear calculations indicate that the critical line is a barrier to meridional propagation so that the tropics should be relatively free of midlatitude influence, and the midlatitudes of each hemisphere should behave essentially independently.

The reciprocal problem, the influence of tropical disturbances on the circulation of the midlatitudes, has also received considerable attention. For example, Webster (1972) was able to show that large-scale slowly varying motions in the zonal mean easterlies of the tropical atmosphere primarily consist of equatorially *trapped* modes. Such modes do not possess a meridional component to their group velocity and their influence is confined to the latitude band of their forcing. Only in special circumstances when the forcing lies partially in the *weak* subtropical zonally-symmetric westerlies can a significant response at higher latitudes occur. Depending upon the characteristics of the higher-latitude zonal flow this response may be substantial (Webster, 1981, 1982; Hoskins and Karoly, 1981).

If the arguments presented above apply to the real atmosphere, tropical motions must be considered to develop *in situ* and would thus be independent of

¹ Contribution No 606, Department of Atmospheric Sciences, University of Washington, Seattle.

large-scale extratropical disturbances. Furthermore, the independence of the two midlatitude zones inferred from the above studies would suggest that the equator is a natural boundary for midlatitude numerical weather prediction models.

However, there appears to exist considerable observational evidence of dynamic links between the midlatitude regions and the tropics and, possibly, between the extratropical regions of the two hemispheres. For example, Radok and Grant (1957) found a relationship between events in the upper tropospheric westerlies in the Australian sector and events to the north of the equator during the Northern Hemisphere winter. Tucker (1965) found evidence of strong cross-equatorial zonally-averaged momentum fluxes in a long data series from a number of tropical stations. Furthermore his analysis indicated substantial longitudinal variation in the time-averaged zonal wind structure; generally, the upper troposphere of the Western Hemisphere was characterized by weak westerly winds while the Eastern Hemisphere was dominated by strong easterlies. These results have been substantiated by Newell *et al.* (1972).

More recent studies suggest significant regionality in the latitudinal interaction. The detailed mean monthly analyses of Sadler (1975) indicate large-scale systems with interhemispheric structure with considerable variability from month to month over the eastern Pacific Ocean. In a study using the Éole balloon data from the upper troposphere of the Southern Hemisphere, Webster and Curtin (1975) indicated a tendency for large-scale slowly propagating middle-latitude troughs to develop severe southeast to northwest horizontal tilts especially in the Pacific Ocean region, implying substantial momentum fluxes out of the tropics. Using NMC data, Murakami and Unninayar (1977) compiled sets of statistics for the upper troposphere including the distribution of perturbation kinetic energy (i.e., the kinetic energy of motions of time scales less than the averaging period; in this case, one month). Sample distributions for January and February 1971 are shown in Fig. 1. Three regions of perturbation kinetic energy maximum are apparent in each diagram. Two regions appear associated with the middle-latitude transient disturbances in each hemisphere while the third exists in a restricted region of the tropics in the eastern Pacific Ocean. A weaker band appears to exist over the tropical Atlantic Ocean. For comparison, the zero line of the mean Northern Hemisphere 200 mb zonal velocity field for the December, January and February period (from Newell *et al.*, 1972) is superimposed on Fig. 1. It is clear that the equatorial perturbation kinetic energy maxima occur in the regions of time-mean zonal westerlies. It is interesting to test the constancy of the longitudinal variation of the zonal wind field throughout the year.

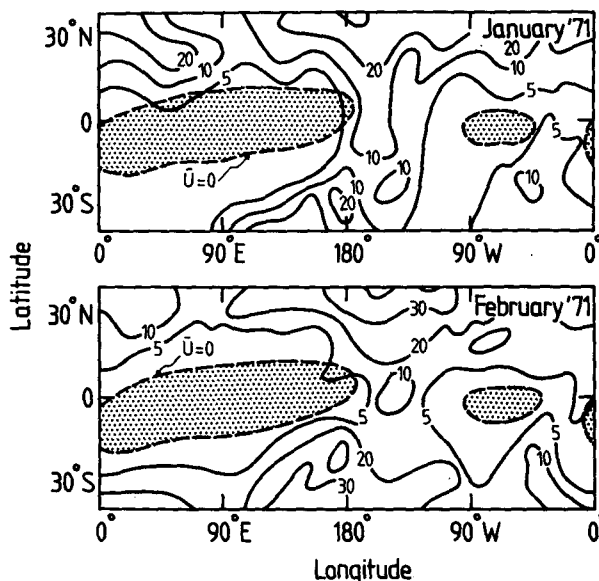


FIG. 1. The 200 mb perturbation kinetic energy distribution ($\text{m}^2 \text{s}^{-2}$) for January and February 1971. The stippled area enclosed in the heavy dashed lines denotes the regions of mean easterly winds. Data obtained from Murakami and Unninayar (1977) and Newell *et al.* (1972).

Fig. 2 shows the annual variation of the monthly mean zonal winds for three meridians; 150°E , 180° and 150°W , adapted from the analyses of Sadler (1975). The first represents the variation in the vicinity of Asia and exhibits strong easterlies throughout the year. However, in the eastern Pacific Ocean westerlies prevail all year and are in excess of 10 m s^{-1} from September to April.

The zones of perturbation kinetic energy could result from disturbances developing *in situ* or from meridionally propagating transient disturbances generated at higher latitudes. It should be remarked that the latter hypothesis is inconsistent with the propagation theory of Charney (1969). Despite the distinct longitudinal structure in the time-mean zonal velocity component, the zonally averaged zonal wind is easterly at low latitudes. However Fig. 1 shows a distinct correlation between positive time-mean zonal winds and the concentration of perturbation energy. Thus, it is intriguing to speculate that the zones of time-mean westerlies in the equatorial upper troposphere form "ducts" which allow transient waves to propagate between extratropical and tropical regions. Thus a primary purpose of this paper is to investigate whether the relaxation of the zonal symmetry constraint in the assumed basic state flow allows the possibility of regional propagation by providing critical lines which are functions of longitude as well as latitude. We will show that the incorporation of a more realistic longitudinally dependent basic state allows the tropical region to be regarded

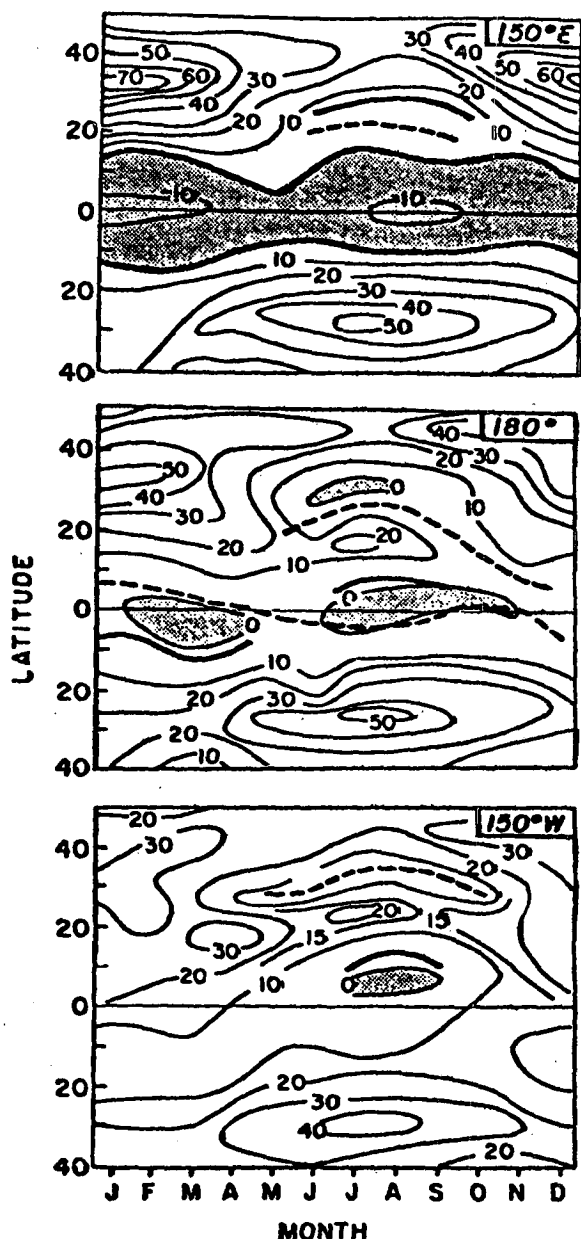


FIG. 2. Annual variation of the mean monthly 200 mb zonal wind distribution along the meridians 100°E , 180° and 150°W adapted from Sadler (1975). The three sections typify the Asian monsoon region, the central Pacific and the eastern Pacific Oceans. Heavy solid and dashed lines indicate 16 positions of the mean troughs and ridges, respectively. Units are m s^{-1} and easterlies are shaded.

as fairly porous, in a regional sense, to incident mid-latitude disturbances.

2. The model

Because we wish to consider basic-state zonal flow fields which are functions of both latitude and longitude it is not possible to obtain analytic solutions

even for the *linearized* response to a specified forcing. An exception is the special case in which the longitudinal scale of the forcing is much less than the scale of the longitudinal variation in the basic state. In that case WKB techniques may be employed for the linear problem. In general, however, a numerical solution is required. Although numerical eigenvalue-eigenfunction techniques could be employed to find solutions to the steady linearized problem, we prefer to utilize a nonlinear initial value technique in order to study the evolution of the response to a "switched on" forcing, and in order to examine the modification to the basic state due to interaction with the forced disturbance.

In order to generate a realistic longitudinally-dependent basic state in the equatorial zone it is essential to include a stationary Kelvin wave component (Webster, 1972). The simplest possible physical model which satisfies this requirement is a barotropic fluid with a free surface (the so-called shallow water equations).²

In the present study the domain of integration is a Mercator projection spanning latitudes $\pm 60^{\circ}$. In Mercator coordinates the momentum equations and continuity equation are

$$u_t - fv + I(u) = -gmH_x - \alpha u, \quad (1)$$

$$v_t + fu + I(v) = -gmH_y - \alpha v, \quad (2)$$

$$H_t + I(H) = M, \quad (3)$$

where the nonlinear terms may be written as

$$I(u) = m(uu_x + vu_y), \quad (4)$$

$$I(v) = m(uv_x + vv_y), \quad (5)$$

$$I(H) = m[(uH)_x + (vH)_y] - Hv_m, \quad (6)$$

where m is the Mercator map factor, and $m = \sec \phi$, where ϕ represents latitude. H represents the depth of the fluid and may be resolved into a zonal mean depth H_0 and a deviation from that mean $h(x, y, t)$ such that

$$H = H_0(y) + h(x, y, t). \quad (7)$$

$M(x, y, t)$ is a specified mass source-sink which will be used to drive the flow. u and v represent the eastward and northward components of velocity and mechanical dissipation is parameterized by Rayleigh friction with a rate coefficient α .

Our numerical model employs a semi-spectral re-

² During final preparation of the manuscript we became aware of the work of Simmons (1981) who has studied the effect of a longitudinally asymmetric basic state in a nondivergent barotropic model. The main emphasis in his work was on the enhancement of the midlatitude response to equatorial forcing due to zonal asymmetries in the strength of the subtropical jet. However, he also noted that cross-equatorial propagation was enhanced when westerlies spanned the equator in a restricted band of longitudes.

presentation in which the variables are expanded in longitudinal eigenfunctions while maintaining a grid point representation in latitude which allows a fine latitudinal resolution. Thus, the variables and the forcing function are expanded in the form

$$\chi(x, y, t) = \sum_{s=0, S} [\chi_s(y, t) \cos sx + \hat{\chi}_s(y, t) \sin sx]. \quad (8)$$

The nonlinear terms are evaluated using the transform method of Orszag (1970): A longitude-latitude grid lattice is chosen to exactly represent the Fourier coefficients. On this grid the nonlinear operators are computed and then Fourier transformed to match the form of (8). That is

$$I[\chi(x, y, t)] = \sum_{s=0, S} [a_s(y, t) \cos sx + \hat{a}_s(y, t) \sin sx]. \quad (9)$$

At each time step the coefficients are thus known quantities so that substituting from (8) and (9) into (1)–(3) we obtain a set of linear equations for the Fourier coefficients

$$u_{st} - fv_s + gmn\hat{h}_s + \alpha u_s = -a_s, \quad (10)$$

$$\hat{u}_{st} - f\hat{v}_s - gmn\hat{h}_s + \alpha \hat{u}_s = -\hat{a}_s, \quad (11)$$

$$v_{st} + fu_s + gmh_{sy} + \alpha v_s = -b_s, \quad (12)$$

$$\hat{v}_{st} + f\hat{u}_s + gm\hat{h}_{sy} + \alpha \hat{v}_s = -\hat{b}_s, \quad (13)$$

$$h_{st} + H_0[mv_{sy} + ms\hat{u}_s - v_s m_y] = M_s - c_s, \quad (14)$$

$$\hat{h}_{st} + H_0[m\hat{v}_{sy} - msu_s - \hat{v}_s m_y] = \hat{M}_s - \hat{c}_s, \quad (15)$$

where a_s, b_s, c_s are coefficients of the transforms of (5)–(7).

Using the semi-implicit time differencing scheme discussed by Holton (1976) and a staggered space-difference scheme in latitude, (10)–(15) become sets of linear algebraic difference equations at each of $K + 1$ latitudinal grid points. The set may be reduced to two algebraic equations at each grid point to produce a total of $2(S + 1)(K + 1)$ sets of simultaneous linear equations which may be solved by matrix inversion.

3. The basic state

We assume that the mean zonal wind (i.e., the zonally symmetric part of the basic-state zonal flow) is initially symmetric about the equator and in geostrophic wind balance with the height field. Thus, in (7)

$$H_0(y) = \bar{H}_{00} + H_b(y), \quad (16)$$

where H_{00} is a constant mean depth, and $H_b(y)$ is related to the longitudinally averaged mean zonal wind $u_b(y)$ geostrophically.

In the atmosphere $u_b(y)$ is maintained by a number of processes which are not included in our simple prototype model. In order to maintain the zonally symmetric "climate" defined by this basic state we assume that the zonal wind relaxes back towards the basic state value by Rayleigh friction damping with the rate coefficient α . Thus, (10) and (11) become

$$u_{st} - fv_s + gmn\hat{h}_s + \alpha(u_s - \delta_0 u_b) = -a_s, \quad (17)$$

and

$$\hat{u}_{st} - f\hat{v}_s - gmn\hat{h}_s + \alpha(\hat{u}_s - \delta_0 u_b) = -\hat{a}_s, \quad (18)$$

where

$$\delta_0 = \begin{cases} 1, & s = 0 \\ 0, & s \neq 0 \end{cases} \quad (19)$$

and $u_b(y)$ is specified as

$$u_b(y) = A - B \cos \frac{\pi}{Ca} (y - y_0), \quad (20)$$

where A, B and C are specified constants and a is the radius of the earth.

The longitudinally varying part of the basic state is obtained by suitable specification of the source-sink term. It is convenient first to split M in (3) such that

$$M = M_b + M_p, \quad (21)$$

where the subscripts b and p indicate the basic and perturbation components of M . We assume a Kelvin wave-like form for M_b which is consistent with both observation and theory for quasi-stationary flow at low latitudes (see Webster, 1972), i.e., we let

$$M_b = B_b \cos s_b x \exp[-y^2/y_1], \quad (22)$$

so that if $u \gg v$ we can use (3) to obtain a scale for B_b . Assuming planetary scales for the basic state ($s_b \sim 1$) we can write

$$M_b \sim B_b \sim H_0(\partial u_b / \partial x) \sim H_0 V / a. \quad (23)$$

We choose y_1 to provide a 1000 km e -folding scale about the equator.

4. Perturbation forcing

A number of experiments were performed to examine the response due to perturbation forcing. Disturbances are introduced by specifying an appropriate form for M_p in (21) such that

$$M_p = B_p f(x) \exp[-(y - y_0)^2/y_2]. \quad (24)$$

Three forms of $f(x)$ were chosen to provide particular isolated mass source-sink distributions over a wide range of scales. These functions are

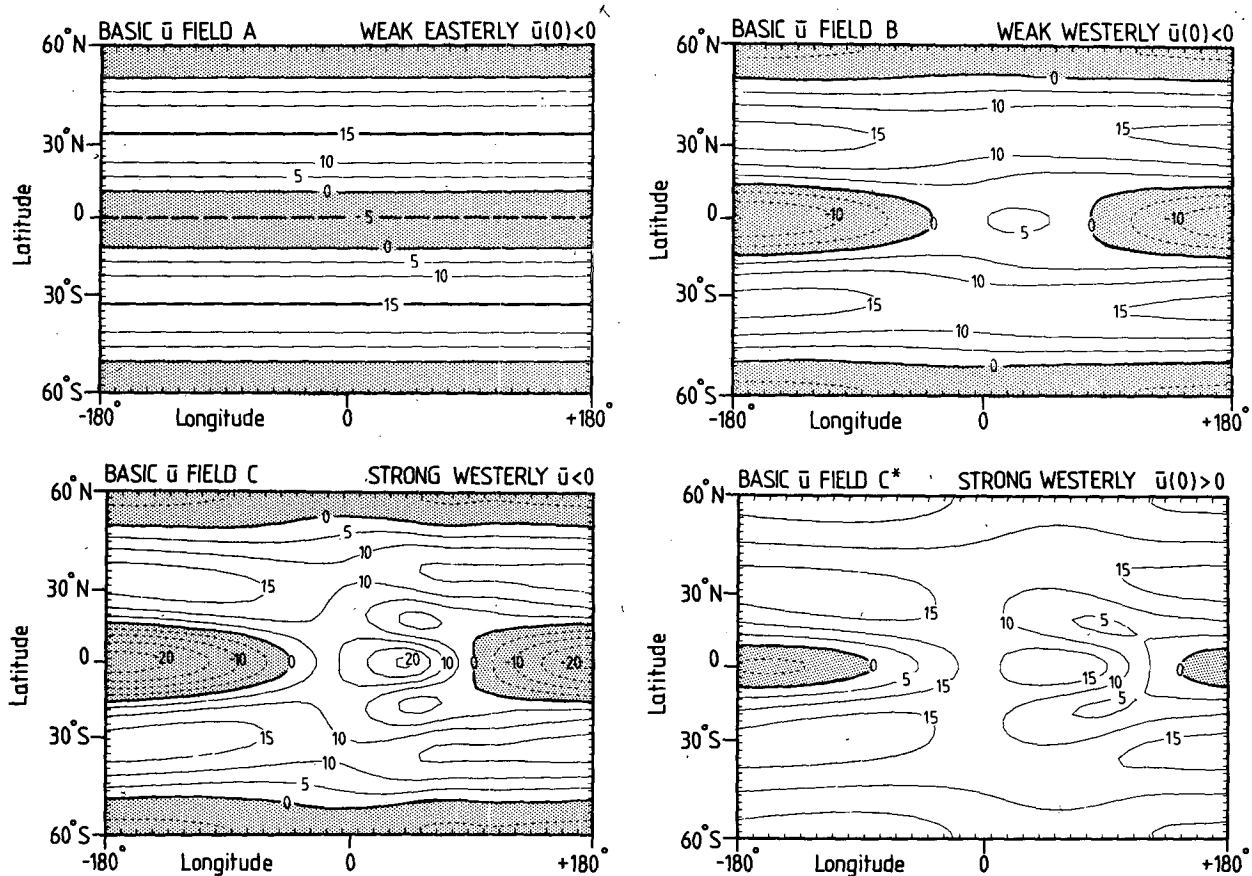


FIG. 3. Distribution of the model-generated basic-state zonal wind field for the "weak easterly" (case A), the "weak westerly" (case B) and the two strong westerly zones (cases C and C*). The stippled areas denote the easterly wind regime. Units m s^{-1} .

$$\left. \begin{aligned} f_1(x) &= \sin(x - x_0) \\ f_2(x) &= \sin(3x - x_0) \\ &\quad \times \exp - 3[(x - x_0)/\pi]^2 \\ f_3(x) &= \sin(6x - x_0) \\ &\quad \times \exp - 6[(x - x_0)/\pi]^2 \end{aligned} \right\} \quad (25)$$

The first function provides a forcing function on the same scale as the longitudinal variation of the basic state. The latter two functions provide dipole forcing functions at scales of the order of the westerly duct in Fig. 2 [i.e., $f_2(x)$] and at scales considerably smaller [$f_3(x)$].³ Specifically, the principal scales are longitudinal wavenumbers 1, 3 and 6. The longitudinal phase of the forcing function is set by x_0 in (25) and the latitudinal location by y_0 in (24). y_2 is set so as to provide a narrow latitudinal scale of 500 km, which is considerably smaller than the e -folding longitudinal scale of the basic state.

³ The exponential dependence in (25) allows a regional isolation of the forcing, thus permitting the longitudinal phase of the forcing to be moved relative to the region of equatorial westerlies.

The latitudinal resolution consisted of 48 grid points (i.e., $K = 48$) and the longitudinal resolution included waves 0–12 (i.e., $S = 12$). In the transformed grid domain of Orszag (1970) this longitudinal wave structure is perfectly represented by a grid of 37 points. That is, in solving for the nonlinear terms a 48×37 lattice was used. Test experiments using $S = 6$ were undertaken and only small differences were found to the $S = 12$ cases. However, we have retained the $S = 12$ resolution to minimize the possibility of spectral blocking.

In all cases presented below the model was initialized to the zonally symmetric basic state and a longitudinally-dependent basic state developed by allowing the basic state forcing (22) to rise from zero to its steady state in the first five days. After ~ 30 days an effective equilibrium was reached but integration was continued to provide a 100-day control run. During all experimental runs the perturbation forcing was introduced at day 50 of the control run with a 5-day growth rate and the model was integrated for a further 50 days. To determine the effect of the forcing the corresponding field of the control run was subtracted from the experiment run to pro-

vide perturbation fields. In all cases a quasi-steady state was achieved well before 100 days.

Experiments were carried out with three major classes of basic state: a zonally symmetric zonal state with weak easterlies in the equatorial region and moderate westerlies elsewhere, an equatorial region possessing a weak westerly wind zone along the equator and an equatorial region characterized by a strong westerly wind zone. The basic state zonal wind fields are shown in Fig. 3. The first case (A) corresponds to the system studied by Charney (1969). The latter two (B and C) are approximations to the more realistic situations described in Figs. 1 and 2. The third state (C) was chosen so that $\langle \bar{u}(y=0) \rangle < 0$. [Here and in the following, angle brackets indicate longitudinal averaging and overbars indicate time averaging.] That is, mean easterlies were maintained at the equator. To consider the effect of relaxing the mean easterly constraint thus allowing $\langle \bar{u}(y=0) \rangle > 0$, the coefficients of (22) were adjusted to produce a fourth basic state C^* .

Each of the four basic states was utilized to study the response to the three perturbation forcing functions described in (25). The basic states and the perturbation forcing format are summarized schematically in Fig. 4. The aim of the experiments is to investigate the influence on the propagation of disturbances of the location and zonal scale of the perturbation forcing relative to the longitudinal position and strength of the equatorial westerly zone. We also investigate how this influence varies with the depth of the prototype atmosphere by varying H_{00} from 1000 to 10 000 m, with 2000 m taken to be the standard depth.

5. Results

a. Weak easterly zone (basic state A)

Fig. 5 shows the perturbation response for the zonally symmetric basic state of Fig. 3a subjected

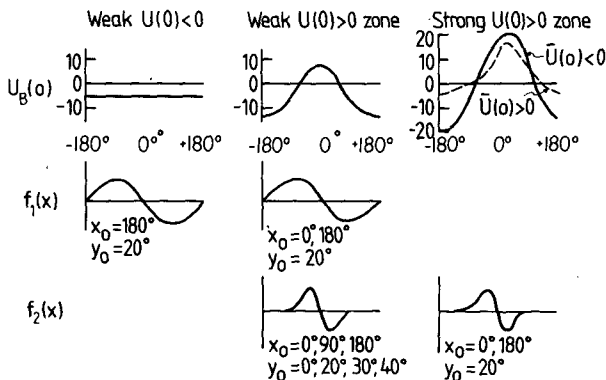


FIG. 4. Schematic diagram of the longitudinal location of the forcing function relative to the extrema of the three classes of the basic state at the equator. Values of x_0 and y_0 refer to forcing function locations used in the experiments.

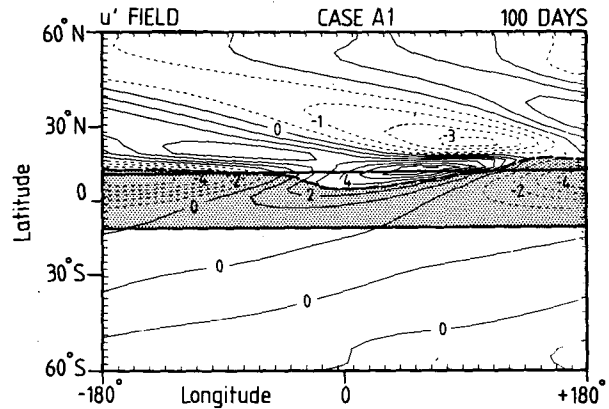


FIG. 5. Distribution of the perturbation zonal wind component (u') at 100 days for an $s = 1$ forcing with $\phi = 0$ located at 20°N (case A1 in Table 1). Basic state A from Fig. 4 was used. The solid heavy lines show the initial $\bar{u} = 0$ contour whilst the heavy dashed lines indicate its final configuration. Contour intervals are 1 m s^{-1} .

to a perturbation source located at 20°N and with an $s = 1$ configuration. In Table 1, this is referred to as case A1 (that is, experiment 1 with basic state A). The form of the basic state is similar to that used by Charney (1969) and Bennett and Young (1971). With the forcing in the Northern Hemisphere, the tropics and Southern Hemisphere remain unperturbed. Only near the $\langle \bar{u} \rangle = 0$ line do significant variations appear. That is, the response is nearly completely confined to the hemisphere of the forcing by the $\langle \bar{u} \rangle = 0$ critical line. The small longitudinally-dependent distortion of the critical line at equilibrium appears to be governed by the phase of the forcing.

b. Weak westerly zone (basic state B)

1) $s = 1$ FORCING

The experiment described above was repeated but with the zonally symmetric basic state replaced by the "weak westerly zone" basic state B of Fig. 3. With this configuration the perturbation forcing function is of larger scale than the zone of westerlies. Because of the scale difference two cases were run: In the first we set $x_0 = 0$ in the definition of f_1 in (25) (case B1), while in the second we set $x_0 = \pi$ (case B2). The u' fields for each case are shown in Figs. 6 and 7, respectively.

Several comparisons are possible: The phase and amplitude of the perturbation forcing function in cases A1 and B1 (shown in Figs. 5 and 6) is the same, thus differences in response must be due to differing basic states. But the difference between cases B1 and B2 on the other hand must originate only from differences in the phase of the perturbation forcing function relative to the zone of weak equatorial westerlies. Despite the common ingredients in the three cases, the equilibrium states indicate dis-

TABLE 1. Summary of the experiments.

Case identifier	Fig.	Basic state Fig. 4	Source function [Eq. (25)]	Source longitude λ	Latitude ($^{\circ}$ N)	Dissipation time (days)
A1	5	A	f_1	0	20	10
B1	6	B	f_1	0	20	10
B2	7	B	f_1	$-\pi$	20	10
B3	9	B	f_2	0	20	10
B4	10	B	f_2	$-\pi$	20	10
B9	11	B	f_2	$-\pi/2$	45	10
C3	12a, b	C	f_2	0	20	10
C3*	13a, b	C*	f_2	0	20	10

tinct differences. In case B1 the zonal velocity field shows a maximum westerly perturbation of $\sim 6 \text{ m s}^{-1}$ just north of the equator and a smaller easterly perturbation to the south of the equator. On the other hand, with $x_0 = \pi$ (case B2) the -8 m s^{-1} change in the zonal wind field centered near the equator has completely eliminated the equatorial westerly zone. There is little or no effect to the south of the equator. In fact, the final equilibrium mean zonal flow is very similar to that shown in Fig. 5. However, we should note that in all three cases in which $s = 1$ the Southern Hemisphere remains relatively unperturbed. At most, case B1 shows a moderate perturbation of the Southern Hemisphere low-latitude region.

The results are summarized in Fig. 8 which shows the latitudinal structure of the perturbation kinetic energy averaged over a 50° longitude strip which passes through the weak westerly zone of basic state B. The profiles for cases A1 and B2 are almost identical. Case B1 shows a substantially greater amplitude in the Northern Hemisphere low latitudes and a profile which is slightly more displaced equatorward than either A1 or B. However, the overriding feature of all three curves is the manner in which rapid decay of amplitude occurs equatorward of the latitude of the $\langle \bar{u} \rangle = 0$ line of the basic zonal flow.

2) $s = 3$ FORCING

The effect of the westerly wind equatorial "duct" becomes more pronounced for waves with smaller zonal scale. Cases B3 and B4 (Figs. 9 and 10) describe the equilibrium fields at day 100 for the $s = 3$ perturbation forcing set at 20° N. The isolated $s = 3$ forcing is located at two positions in longitude; at 0° W in Fig. 9 and 180° W in Fig. 10. Both cases show propagation of the disturbance into the westerlies of the Northern Hemisphere as may be anticipated from Hoskins and Karoly (1981). But only when the forcing is located in the same longitude band as the weak equatorial westerlies is there any propagation towards the equator. This effect may be seen clearly in the u' field of Fig. 9 where substantial perturbations occur in the equatorial region and there is even a weak propagation into the subtropics of the Southern Hemisphere. This is in sharp contrast to the case B4 where there is effectively no equatorial propagation at all. Both cases may be qualitatively understood from a WKB perspective. With strong easterlies to the south of the forcing (B4) the response is constrained to lie poleward of the source. Thus in Case B4 the only changes which occur equatorward of the forcing are small changes in the \bar{u}

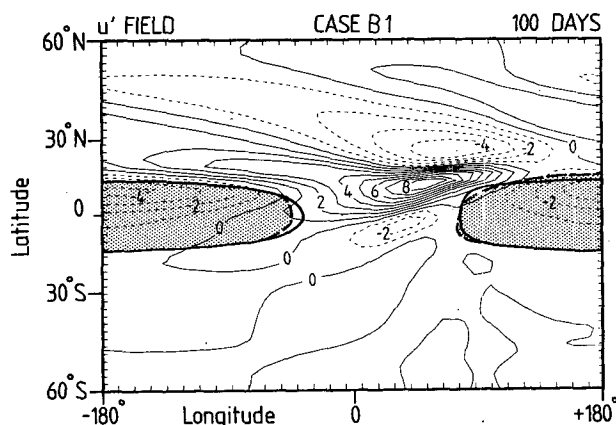


FIG. 6. As in Fig. 5 except for case B1 which considers an $s = 1$ forcing with $\phi = 0$ but relative to an initial basic state B. Contour intervals are halved.

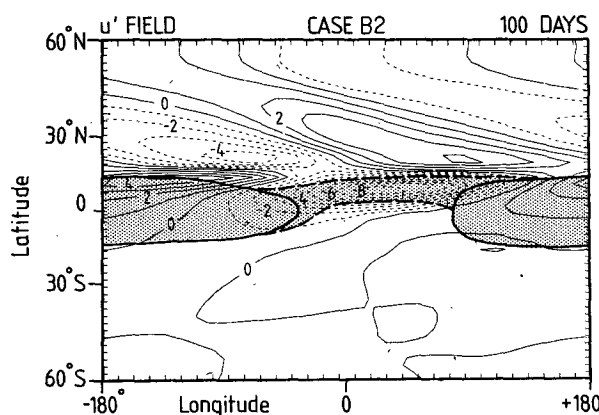


FIG. 7. As in Fig. 5, except for case B2 which considers an $s = 1$ forcing but with $\phi = \pi$ phase difference to case B. The basic state B was used. Contour intervals are halved.

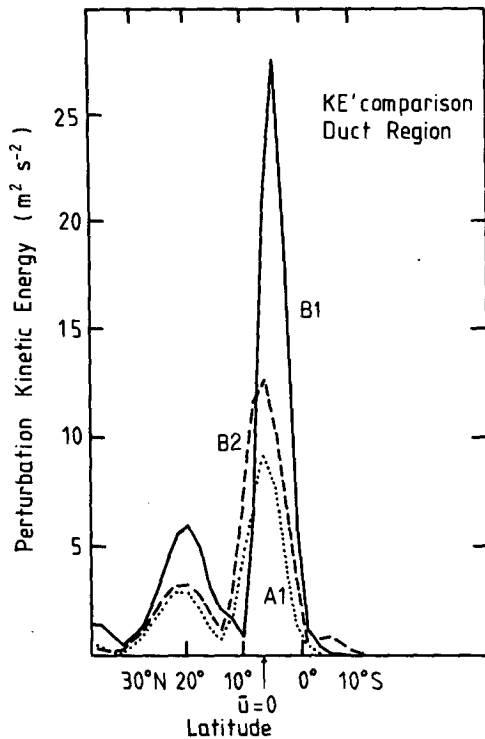


FIG. 8. The distribution of perturbation kinetic energy ($\text{m}^2 \text{s}^{-2}$) shown as a function of latitude for cases A_1 , B_1 and B_2 . The kinetic energy was averaged over a 50° longitude strip through the region of the equatorial westerlies.

= 0 line. However, in Case B3 the weak westerlies near the equator allow a greater penetration towards the equator. Similar $s = 3$ perturbation experiments were run for sources located at 30° and 45°N . In both cases the results were similar to those of the 20°N source (cases B3, B4).

Fig. 11 describes one further forced experiment with the weak westerly basic state. With the $s = 3$

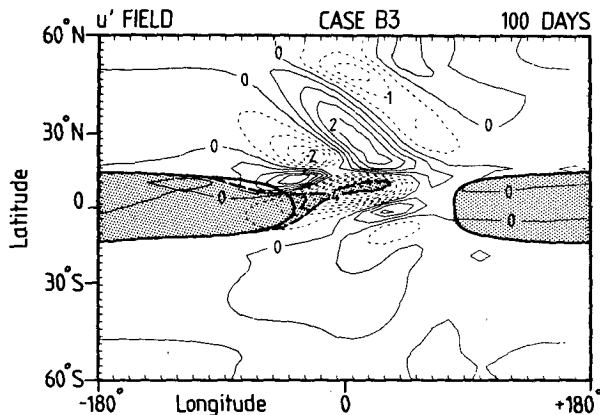


FIG. 9. As in Fig. 5 except for case B_3 which considers an $s = 3$ forcing at 20°N and basic state B. Contour intervals are halved.

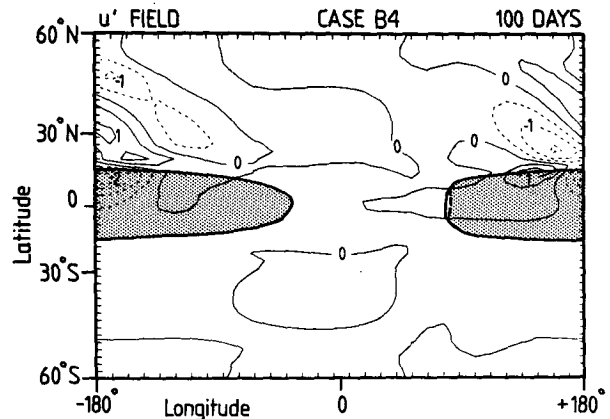


FIG. 10. As in Fig. 5 except for case B_4 which considers an $s = 3$ forcing at 20°N with basic state B but with the forcing moved in longitude. Contour intervals are halved.

forcing set at 45°N , the longitudinal location was moved upstream by $\pi/2$ from the center of the westerly region. The response underlines the importance of the location of the source relative to the equatorial westerlies. Whereas a strong equatorially-propagating wave train is developed, the degree of equatorial influence is restricted by the presence of the basic easterlies.

Although cases B3, B4 and B9 do indicate the importance of longitudinal asymmetries in the basic-state zonal flow, the response in the Southern Hemisphere is certainly too small to account for some of the observed interhemisphere coupling described earlier. One possible explanation for the small response is that the rather short damping time assumed (10 days) does not allow disturbances to propagate far into the Southern Hemisphere.

This hypothesis was tested by an experiment in which all factors were identical to case B3 (isolated $s = 3$ forcing at 20°N directly to the north of the

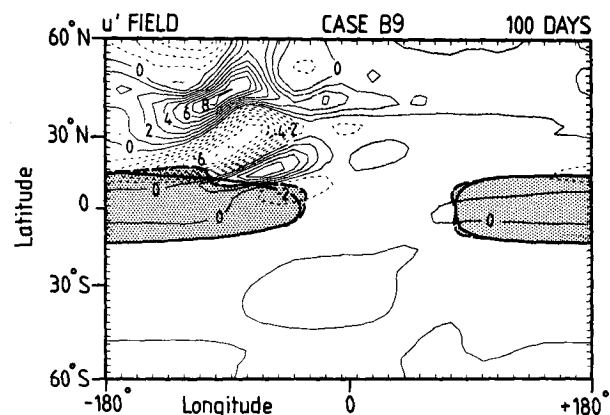


FIG. 11. As in Fig. 5 except for case B_9 which considers an $s = 3$ forcing located at 45°N moved $\pi/2$ in longitude westward with basic state B.

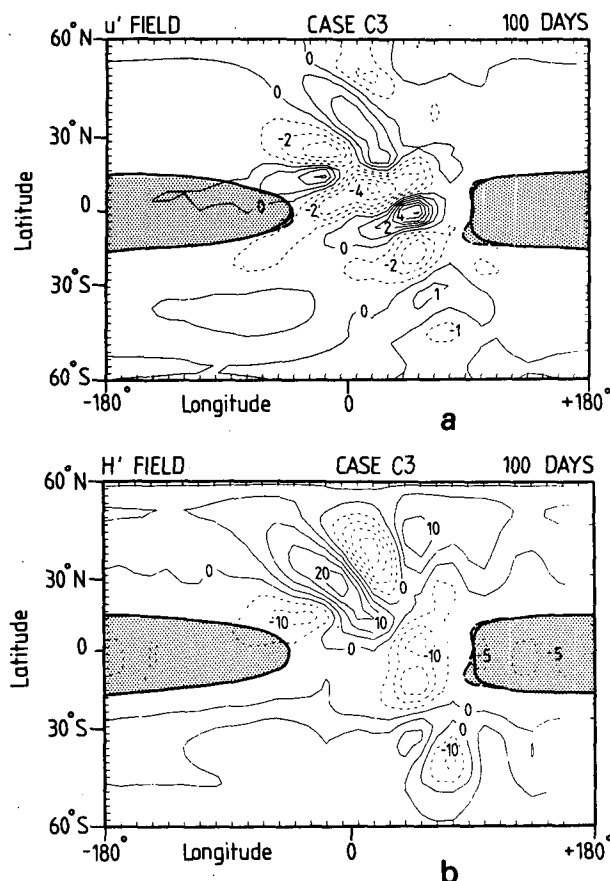


FIG. 12. (a) As in Fig. 5 except for case C₃ which considers an $s = 3$ forcing located at 20°N with basic state C. (b) The perturbation height field (contour interval 5 m).

weak westerlies) except that the dissipation rate has been halved to 20 days. The perturbation zonal velocity (not shown) was considerably stronger in the equatorial regions and, furthermore, increased propagation occurred into the subtropics of the Southern Hemisphere. However, there still appeared to be rather little response in the midlatitudes of the Southern Hemisphere.

c. Strong westerly zone (basic state C)

The response to an isolated $s = 3$ forcing with basic state C is shown in Figs. 12a and 12b. Recall that states A, B and C are similar in that the zonally-averaged zonal velocity component is negative in the equatorial belt. However, in B and C there is a longitudinally-dependent portion of the basic state. C differs from B in that a stronger westerly zone has been produced by a stronger basic state mass source/sink distribution at the equator.

A comparison of cases B3 (Fig. 9) and C3 (Fig. 12) indicates a substantial difference in response. Not only are the perturbation effects at low latitudes considerably larger at the equator in C3, but sub-

stantial propagation has occurred into the middle latitudes of the Southern Hemisphere. It should be pointed out that the scale of the region of equatorial westerlies in basic states B and C is nearly identical.

The case C₃ perturbation height field shown in Fig. 12b indicates very well the meridional extent of the anomalous response. The amplitude of the height perturbations in the Southern Hemisphere is over 50% of that in the Northern Hemisphere midlatitudes. Also, the height perturbations in the strong equatorial westerlies are extremely large and correspond in longitude to the maximum in the equatorial westerlies. This probably indicates the generation of a substantial equatorial mode.

To gain some insight into the importance of the $\langle \bar{u} \rangle < 0$ constraint at low latitudes a modified basic state (C*) was established which allowed $\langle \bar{u} \rangle > 0$ at the equator. The maximum in the westerlies at the equator (18 m s^{-1}) is much the same as the 20 m s^{-1} for state C. The major differences between the two states is that the region of westerlies in C* is somewhat broader in longitudinal scale, and the zonal average of the zonal wind is positive everywhere.

The equilibrium response of the state C* to the isolated $s = 3$ forcing at 20°N (Fig. 13) is quite similar to case C₃; large amplitude responses are evident at low latitudes and in the Southern Hemisphere, although the magnitude of the height perturbation at the equator is about a factor of four smaller. We conclude that for $s = 3$ the scale of the disturbance is small enough so that the disturbance can propagate through the equatorial westerly jet without respect to the existence of a mean zonal $\langle \bar{u} \rangle = 0$ critical line. Experiments with perturbation forcing of smaller scale ($s = 6$) showed results very similar to the $s = 3$ case, and will not be discussed further here.

6. Interpretations

The results confirm observational indications of linkages between disturbances in the middle latitudes of one hemisphere, the adjacent regions near the equator and the middle latitudes of the other hemisphere. The observations indicate that the zones of coupling are restricted to corridors of climatological low-latitude westerlies, and the model results tend to confirm this.

Returning to the hypotheses posed in the Introduction, we may single out a number of aspects of the results which require particular discussion and interpretation. These are:

1) *Large-scale disturbances generated in the middle latitudes of one hemisphere have little effect on low latitudes when there exists a $\langle \bar{u} \rangle = 0$ line between the source and the equator.*

Experiments using the zonally-symmetric basic

state A (see Figs. 4 and 5) confirm results of Charney (1969) and Bennett and Young (1971), that a critical line for stationary disturbances (i.e., the $\langle \bar{u} \rangle = 0$ line) acts as an effective barrier or separator between the tropics and middle latitudes. If the mean state of the atmosphere were represented by a zonally-symmetric distribution of mean wind characterized by equatorial easterlies and middle-latitude westerlies, then all equatorial disturbances would have to be generated *in situ* and in turn, would have little effect on middle-latitude structures.

It must be emphasized that it is the existence of a $\langle \bar{u} \rangle = 0$ line which is most important in the *zonally-symmetric atmosphere* and not the latitude of the forcing or region of response. If the distribution of zonally symmetric westerlies was such that the westerlies extended across the equator, then the two-dimensional group velocity vector of the Rossby waves excited in middle latitudes would cause considerable perturbation at low latitudes and in the westerlies of the Southern Hemisphere (see case T3 of Webster, 1973). If the basic state is characterized by easterlies extending from the equator northward and including the perturbation source region, the response at low latitudes will be limited to the equatorial plane because only equatorially-trapped modes would be excited.

2) *Large-scale disturbances generated in the middle latitudes of one hemisphere may have a significant influence on the equatorial regions and the higher latitudes of the other hemisphere if in some longitude zone a westerly wind duct exists in the equatorial zone.*

With basic states B and C a distinct propagation across the equator was observed in the model results for modes of planetary wavenumber 3 or greater. The region of propagation coincided with the equatorial westerlies; regions of equatorial easterlies were unperturbed irrespective of the location of the forcing. These results may be understood in terms of the theory of propagation of Rossby modes on a sphere (e.g., Hoskins and Karoly, 1981). Rossby modes excited in the westerlies will possess ray paths which branch on great circle paths poleward and equatorward from the source. Thus for scales of motion considerably smaller than the basic-state scale (so that the WKB approximation is valid), motions excited to the north of the equatorial westerlies will propagate to the equator whereas those excited to the north of the easterlies will be retarded at the local critical latitude. In both instances (see Figs. 9 and 10) propagation takes place on the poleward branch, but only when the raypath of the excited mode passes through the westerly duct can the disturbance propagate into the Southern Hemisphere.

3) *The amplitude of the response in the equatorial zone and in the opposite hemisphere depends*

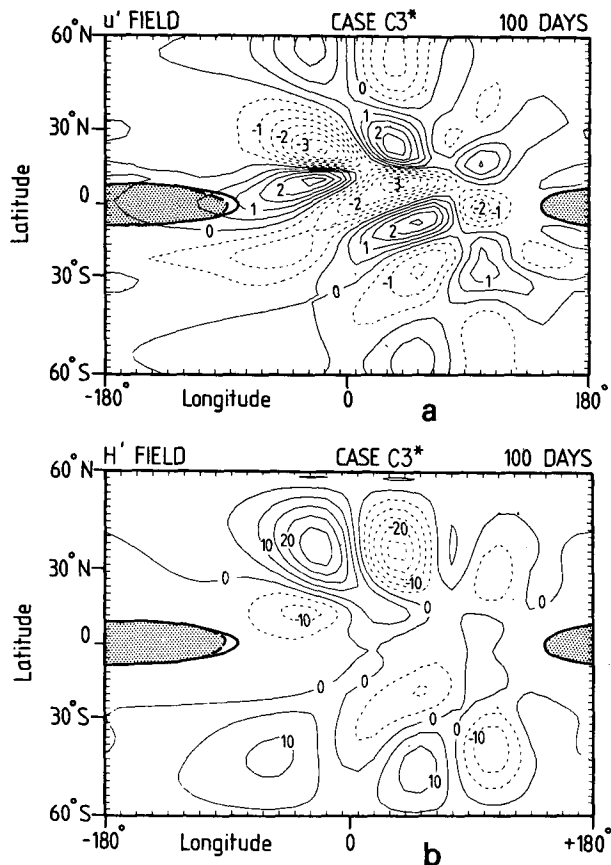


FIG. 13. As in Fig. 12 except for case C_3^* which considers an $s = 3$ forcing located at 20°N . As distinct from case C_3 , the basic state used possessed a zonally symmetric part which was westerly at the equator. Both cases possessed the same longitudinal part of the basic zonal wind field.

strongly on the magnitude of the westerlies in the equatorial duct.

This strong dependence can be understood quite simply in terms of the dispersion characteristics of forced Rossby waves. For the parameters of these experiments the disturbance excited by the perturbation source can be reasonably well approximated by nondivergent Rossby modes.⁴ The only exception is case B6 in which the source is located at the equator and a substantial divergent equatorial mode is generated.

The dispersion relation for a barotropic Rossby wave can be written (e.g., Holton, 1979) as

$$\omega/k = \bar{u} - \beta/(k^2 + l^2), \quad (26)$$

where ω is the frequency, $\beta \equiv 2\Omega/(\cos\phi a)$; k and l

⁴ For the equivalent depth $H_{00} = 2000$ m, used here, divergence associated with fluctuations of the free surface height causes only a small modification in the Rossby wave dispersion relationship. (Experiments similar to case B3 but with H_0 varied from 1000 to 10 000 m differed very little from case B3.)

TABLE 2. Dependence of stationary Rossby-wave group velocity on the mean zonal wind. L_y indicates the meridional e -folding decay scale for 10-day damping time.

\bar{u} (m s^{-1})	l (m^{-1})	c_{gx} (m s^{-1})	c_{gy} (m s^{-1})	L_y (km)
5	2.1×10^{-6}	0.5	2.1	1854
10	1.4×10^{-6}	1.9	5.9	5098
15	1.1×10^{-6}	4.3	10.5	9072
20	9.6×10^{-7}	7.7	15.8	13651

are the zonal and meridional wavenumbers and \bar{u} is here considered to be slowly varying in longitude. If k and \bar{u} are known, then for stationary modes,

$$l^2 = \beta/\bar{u} - k^2. \quad (27)$$

Using (27) we can solve for the components of the horizontal group velocity

$$\left. \begin{aligned} c_{gx} &\equiv \partial\omega/\partial k = \bar{u} - \beta(l^2 - k^2)/(k^2 + l^2)^2 \\ c_{gy} &\equiv \partial\omega/\partial l = 2\beta kl/(k^2 + l^2)^2 \end{aligned} \right\} \quad (28)$$

As a result for stationary perturbations we find using (27) that

$$c_{gx} = 2\bar{u}^2 k^2 / \beta, \quad (29)$$

$$c_{gy} = 2\bar{u}^2 kl / \beta \simeq 2\bar{u}^{3/2} k / \beta^{1/2}, \quad (30)$$

where the approximate formula in (30) is valid provided $\beta/\bar{u} \gg k^2$, which is the case for scales of interest here. From (29) and (30) it is clear that for a given zonal scale k , both components of the group velocity increase rapidly with \bar{u} . The zonal scale of the primary resonant response should be equal to the zonal scale of the forcing. Thus, for our cases B3, B4, B6 and C3 we set $k = 3/a$, corresponding to wavenumber 3 at the equator. Table 2 shows the resulting dependence of group velocity on \bar{u} for β evaluated at the equator.

For $\bar{u} = 5 \text{ m s}^{-1}$ energy can propagate only 1800 km meridionally away from the source in 10 days (the e -folding decay time in all experiments except B3*). However, for $\bar{u} = 15 \text{ m s}^{-1}$ energy can propagate over 9000 km meridionally in 10 days. Thus, assuming that the wavenumber 3 disturbance excited by the source "sees" the local zonal wind in the westerly duct as the "mean" wind, it becomes clear why strong perturbations are excited in the Southern Hemisphere in the strong westerly case (C3) but not in the weak westerly case (B3). In the latter case dissipation simply damps the disturbance out before it can reach far into the Southern Hemisphere.

7. Concluding remarks

Inter-hemispheric interaction is obviously important for time scales ranging from short-range numerical weather prediction to climatic variations. For numerical weather prediction, knowledge of the interaction is necessary for specifying equatorial

boundary conditions and also as an aid in deciding to what degree of sophistication the tropics must be treated for a forecast of a particular duration. For climate, it is critical to understand disturbance transmission in a longitudinally-dependent basic state in order to determine regions of influence from (e.g.) sea-surface temperature anomalies located at various longitudes at low latitudes. It is also important to understand the role of such anomalies in exciting and maintaining longitudinal asymmetries in the basic state.

The results of this study have some interesting implications for numerical weather prediction. If the strong meridional propagation through the equatorial westerly duct seen in the model is characteristic of the atmosphere, then rapid local contamination of hemispheric forecasts could occur due to noise generated in the opposite hemisphere propagating through a westerly duct. Thus, when local regions of strong equatorial westerlies exist, the domain of influence for hemispheric forecasts beyond 2–3 days must include at least the subtropics of the opposite hemisphere. Of course the motions in the tropical region itself would need to be accurately forecast in order to correctly predict the meridional wave propagation through the duct.

The sensitivity of the model results to the strength of the equatorial westerlies implies that interhemispheric interaction should have an annual variation since, as shown in Fig. 2, the magnitude of the westerlies in the equatorial region of the Eastern Pacific is strongest ($>15 \text{ m s}^{-1}$) in the October–May period. Thus the strongest interhemisphere coupling in this region should occur in the Northern Hemisphere winter.

Our study also appears to be relevant to understanding some aspects of low frequency (interannual) variability. Webster (1981, 1982) and Hoskins and Karoly (1981) have shown that the teleconnection patterns associated with Rossby waves excited by equatorial diabatic heating anomalies are sensitive to the basic-state zonal wind field. Thus, the character of such patterns should depend sensitively on the location and strength of any equatorial westerly wind duct. To a large extent the climatological mean state of the tropical atmosphere depends on the tropical sea-surface temperature distribution. Thus, during El Niño periods interhemispheric interactions due to meridional wave propagation should be strongly affected. Similarly, wave trains excited in midlatitudes (e.g., by topographic forcing) may be reflected at a tropical critical line or propagate into the opposite hemisphere depending on the zonal wind distribution in the tropics. [The occurrence of such reflection requires that the critical line dynamics be nonlinear. A linear critical line would absorb rather than reflect.]

The equatorial westerly duct may also account for some of the low-frequency variability seen at higher

latitudes. Lau (1981) has shown using a long time series generated by the GFDL spectral general circulation model that there exist a few "centers of low frequency action" in the Northern Hemisphere. As the boundary forcing in the model had only an annual cycle, Lau interpreted the interannual variability in the model as resulting from natural randomness of the system.

One of Lau's centers of low frequency variability is in the Eastern North Pacific Ocean in agreement with observations. Most workers have interpreted this variability in the atmosphere as resulting from meridional propagation of wave modes excited by equatorial sea-surface temperature anomalies (Webster, 1981b), although this mechanism seems to contribute only ~30–40% of the total observed variance. However, it should be noted that this region of strong interannual variability lies poleward and eastward of the equatorial westerly duct. Consequently, Lau's centers of low-frequency variability may be coupled in some manner to low-frequency or transient features of the opposite hemisphere whose influence waxes and wanes with the seasonal variability of the equatorial westerly duct.

Although many aspects of the problem remain unexplored, we can state with some confidence that the interhemispheric response depends primarily on *the strength of the local westerlies at the equator rather than whether the zonally-averaged zonal wind component at low latitudes is negative or positive*. This probably means that except for planetary-scale modes, we must reconsider the concept of a critical latitude and substitute the concept of a longitudinally varying critical line. The problem is in some ways analogous to the vertical wave propagation problem. Just as in that case, where the vertical group velocity must be considered in conjunction with the zonal group velocity, it would appear that here we must consider the meridional group velocity component.

Finally it should be noted that the inferences we have drawn concerning cross-equatorial propagation in the real atmosphere require consideration of the full atmospheric spectrum of transient wave phase speeds. Our discussion has implicitly assumed that the waves are zonally stationary ($c = 0$). However, the arguments given should hold equally well if we consider the critical line $\bar{u} - c = 0$ where the Doppler-shifted phase speed vanishes.

Acknowledgments. This research was carried out in part while one of us (JRH) was a visiting scientist at the CSIRO Division of Atmospheric Physics, Melbourne. We wish to thank Dr. Brian Tucker, Chief of the Division, for his hospitality in facilitating this visit. The computer graphics were handled by Mr. Peter Brenten. This research was supported in part by the National Science Foundation, At-

mospheric Research Section, under Grant ATM79-24687.

REFERENCES

- Beland, M., 1976: Numerical study of the nonlinear Rossby wave critical level development in a barotropic zonal flow. *J. Atmos. Sci.*, **33**, 2065–2078.
- Bennett, J. R., and J. A. Young, 1971: The influence of latitudinal wind shear upon large-scale wave propagation into the tropics. *Mon. Wea. Rev.*, **99**, 202–214.
- Charney, J. G., 1963: A note on large scale motions in the tropics. *J. Atmos. Sci.*, **20**, 607–609.
- , 1969: A further note on large scale motions in the tropics. *J. Atmos. Sci.*, **26**, 182–185.
- Dickinson, R. E., 1970: Development of a Rossby wave critical level. *J. Atmos. Sci.*, **27**, 627–633.
- Geisler, J. E., and R. E. Dickinson, 1974: Numerical study of an interacting Rossby wave and barotropic zonal flow near a critical level. *J. Atmos. Sci.*, **31**, 946–955.
- Holton, J. R., 1976: A semi-spectral numerical model for wave-mean flow interactions in the stratosphere: Application to sudden stratospheric warmings. *J. Atmos. Sci.*, **33**, 1639–1649.
- , 1979: *An Introduction to Dynamic Meteorology*. Academic Press, 391 pp.
- Hoskins, B. J., and D. J. Karoly, 1981: The steady linear response of a spherical atmosphere to thermal and orographic forcing. *J. Atmos. Sci.*, **38**, 1179–1196.
- Lau, N.-G., 1981: A diagnostic study of recurrent meteorological anomalies appearing in a 15-year simulation with a GFDL general circulation model. *Mon. Wea. Rev.*, **109**, 2287–2311.
- Mak, M.-K., 1969: Laterally driven stochastic motions in the tropics. *J. Atmos. Sci.*, **26**, 41–64.
- Murakami, T., and M. S. Unninayar, 1977: Atmospheric circulation during December 1970 through February 1971. *Mon. Wea. Rev.*, **105**, 1024–1038.
- Newell, R. E., J. W. Kidson, D. G. Vincent and G. J. Boer, 1972: *The General Circulation of the Tropical Atmosphere and Interactions with Extratropical Latitudes*, Vol. 1. MIT Press, 258 pp.
- Orszag, S. A., 1970: Transform method for the calculation of vector coupled sums: Application to the spectral form of the vorticity equation. *J. Atmos. Sci.*, **27**, 890–895.
- Radok, U., and A. M. Grant, 1957: Variations in the high tropospheric flow over Australia and New Zealand. *J. Meteor.*, **14**, 141–149.
- Sadler, J., 1975: The upper tropospheric circulation over the global tropics. Tech. Rep. UHMET-75-05, Dept. Meteor., University of Hawaii, 35 pp.
- Simmons, A. J., 1981: The forcing of stationary wave motion by tropical diabatic heating. Submitted to *Quart. J. Roy. Meteor. Soc.*
- Tucker, G. B., 1965: The equatorial tropospheric wind regime. *Quart. J. Roy. Meteor. Soc.*, **91**, 140–150.
- Tung, K. K., 1979: A theory of stationary long waves, Part III: Quasi-normal modes in a singular wave guide. *Mon. Wea. Rev.*, **107**, 751–774.
- Warn, T., and H. Warn, 1978: The evolution of a nonlinear Rossby wave critical level. *Stud. Appl. Math.*, **59**, 37–71.
- Webster, P. J., 1972: Response of the tropical atmosphere to local steady forcing. *Mon. Wea. Rev.*, **100**, 518–540.
- , 1973: Remote forcing of the time-independent tropical atmosphere. *Mon. Wea. Rev.*, **101**, 58–68.
- , 1981: Mechanisms determining the atmospheric response to sea surface temperature anomalies. *J. Atmos. Sci.*, 554–571.
- , 1982: Seasonality in the local and remote atmospheric response to sea surface temperature anomalies. *J. Atmos. Sci.*, **39**, 41–52.
- , and D. G. Curtin, 1975: Interpretations of the EOLE experiment II. Spatial variation of transient and stationary modes. *J. Atmos. Sci.*, **32**, 1848–1863.